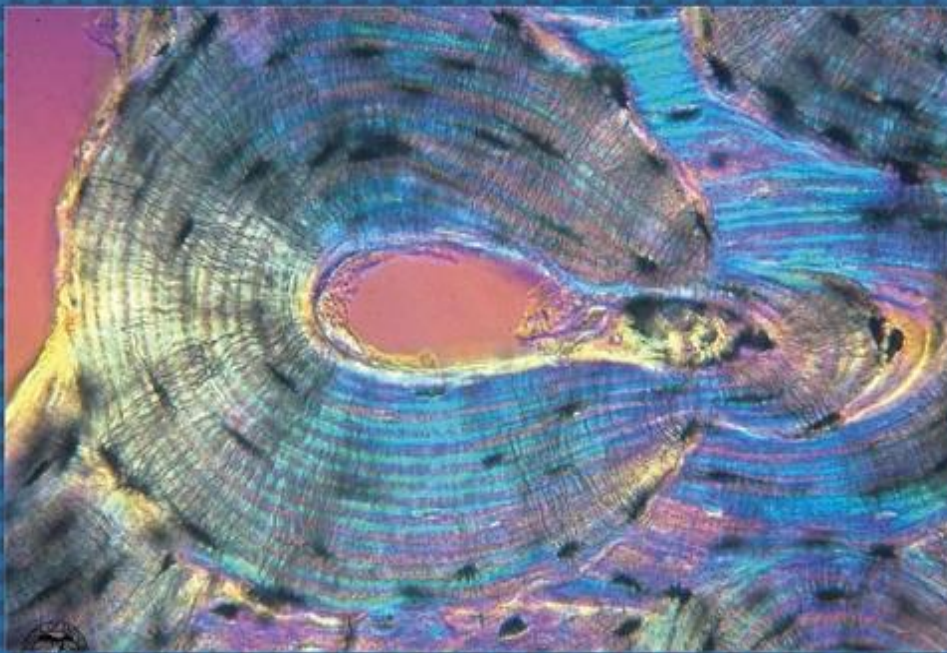




EGYPTIAN ACADEMIC JOURNAL OF
BIOLOGICAL SCIENCES
HISTOLOGY & HISTOCHEMISTRY

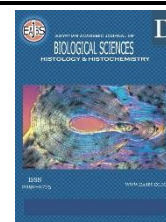
D



ISSN
2090-0775

WWW.EAJBS.EG.NET

Vol. 14 No. 2 (2022)



Adipose Tissue-Mesenchymal Stem Cells Improve Cisplatin-Induced Cardiotoxicity in Rats Via Modulating Apoptosis, Oxidative Stress, Inflammation, and Angiogenesis

Amal Rateb^{1,*}, Asmaa M.S. Gomaa² and Ola A. Hussein³

1-Human Anatomy and Embryology department, faculty of Medicine, Assiut University – Assiut 71515, Egypt.

2-Department of medical physiology, Faculty of Medicine, Assiut University, Assiut 71515, Egypt.

3-Department of Histology and Cell Biology, Faculty of Medicine, Assiut University, Assiut 71515, Egypt.

E.Mail*: Amal.badi@med.aun.edu.eg-asmaasayed@aun.edu.eg-olaa.2012@aun.edu.eg

ARTICLE INFO

Article History

Received:2/9/2022

Accepted:2/11/2022

Available:6/11/2022

Keywords:

Cardiotoxicity;

caspase-3;

Cisplatin;

Oxidative stress;

Stem cells; TNF-

α ; VEGF.

ABSTRACT

Background: Cardiotoxicity is a common adverse reaction to cisplatin treatment. Not all the mechanisms underlying cisplatin-induced cardiotoxicity have been described. Stem cells have been acknowledged as a potentially effective, novel treatment approach in treating several diseases.

Objective: The current study was done to assess the impact of adipose mesenchymal stem cells (ADMSCs) in repairing cardiac damage induced by cisplatin and to investigate the underlying mechanisms. **Materials and Methods:** 32 rats were utilized for this study. They were randomly classified into four equal groups: the Control group that received saline intraperitoneally (i.p.), the Cisplatin-treated group that received a single i.p. injection of cisplatin at a dose of 7 mg/kg and was left for 5 days, Stem cell-treated group that administered cisplatin as before and after 5 days they received a single dose of ADMSCs (1×10^6) mL injected intravenously and were left for 60 days after cell injection, and the Withdrawal group that received cisplatin in same dose and manner of administration as above and then left for 65 days. At the end of the experiment, the portions of the heart specimen were used to determine the levels of Total antioxidant capacity (TAC), cardiac Malondialdehyde (MDA), Tumor nuclear factor- α (TNF- α), and interleukin 2 (IL-2). The remaining portions of the heart muscle were prepared for histological and immunohistochemistry studies.

Results: Cisplatin treated group revealed extensively disrupted organization of muscle fibers that appeared remarkably damaged with focal lysis with the widening of the spaces among the myofibrils, severely distorted nuclei which appeared highly condensed and had irregular malformed shapes with severe mitochondrial changes. Also, the levels of proinflammatory cytokines e.g., TNF- α and IL-2 were increased in the cardiac tissue. Also, increased MDA and decreased TAC levels were detected. Injection of ADMSCs ameliorated cardiotoxicity induced by cisplatin via suppression of oxidative injury, inhibition of pro-inflammatory cytokines, suppression of apoptotic cascades, and activation of angiogenesis. **Conclusion:** This study could be considered preliminary in proving that AD-MSCs therapy has a promising role to enhance marked regeneration of cisplatin-induced myocardial injury.

INTRODUCTION

Cisplatin is one of the common clinical chemotherapeutic drugs. Despite high efficiency, several studies proved that it is accompanied by numerous side effects, such as nephrotoxicity, myelotoxicity, gastrointestinal toxicity, neurotoxicity, and cardiotoxicity (Sherif, Abdel-Aziz, *et al.*, 2014, Martínez-Mateo, Anguita *et al.*, 2017). Cardiotoxicity is a common adverse reaction to cisplatin treatment. Some patients suffered a myocardial infarction, angina pectoris, and abnormal diastolic function of the left ventricle. Moreover, an electrocardiogram (ECG) showed signs of transmural ischemia of the heart, and an echocardiogram demonstrated irreversible myocardial damage (Lian, Gao *et al.*, 2016).

The mechanism of cardiotoxicity induced by cisplatin is not well illustrated, although oxidative stress activation inducing apoptosis and cell death has been postulated and has received the most attention (Varga, Ferdinandy *et al.*, 2015, Varricchi, Ameri *et al.*, 2018). Furthermore, oxidative stress is involved in the induction of elevated levels of cytokine tumor necrosis factor- α (TNF- α) (Chowdhury, Sinha *et al.*, 2016).

Stem cells have attracted a lot of interest as a potentially effective, novel therapeutic approach for treating many disorders (Večerić-Haler, Cerar *et al.*, 2017). Endogenous regenerating cardiac stem cells were first proposed in 2001 (Maliken and Molkentin 2018). Stem cells can be used to heal tissues from ROS-damaging effects because of their antioxidative properties (Kobayashi and Suda 2012, Hassan and Alam 2014). Considering this, stem cells could be new therapeutic hope for patients suffering from cisplatin-induced cardiotoxicity.

New myocytes might be produced by adult cardiac and mesenchymal stem cells that expressed

the protein (c-kit) (Beltrami, Barlucchi *et al.* 2003, Marra, Bizzarro *et al.* 2004). According to these findings, progenitor cells can go to the site of an injury and develop into cardiac cells (Huang, Zhang *et al.*, 2010). Additionally, some research (Pelacho, Aranguren *et al.*, 2007, Mathur, Fernández-Avilés *et al.*, 2017) looked into the potential of regenerative medicine as a substitute for heart transplantation. It is evident that mesenchymal stem cells (MSCs) are an appropriate choice for preventing and treating myocardial diseases. Because they are simpler to be isolated from subcutaneous adipose connective tissue and are easier to retrieve, adipose-derived mesenchymal stem cells (ADMSCs) are viewed as a more viable treatment option than bone marrow-derived cells (BM-MSCs). Additionally, they have a strong proliferative potential and produce a large number of cells (Mazini, Rochette *et al.*, 2019). Besides the successful use of MSCs in animal models of various organ toxicity (Abushouk, Salem *et al.*, 2019) and to the best of our knowledge, no previous study dealt with this topic; we have been urged to conduct the present study in order to evaluate how adipose-MSCs counteract the cardiac damage brought on by cisplatin and to look into any potential protective mechanisms.

MATERIALS AND METHODS

1. Animals:

32 adults male Wistar Albino rats, 8 weeks old, weighing 150–180 g, were used in this study. The animals were from the Animal Laboratory House of the Faculty of Medicine at Assiut University. The experimental protocol of the Faculty of Medicine at Assiut University in Assiut, Egypt, was approved by the Institutional Committee. They were cared for in accordance with the National Institutes of Health's guide for the care and use of Laboratory animals (NIH Publications No. 8023, revised 1978). Throughout the experiment, animals had full access to a

well-balanced feed and tap water as well as typical housing circumstances, including suitable temperature and a natural photoperiod. After acclimatization for a week, randomly the animals were divided into four equal groups.

2. Chemicals and Drugs:

Mylan provided cisplatin vials (50 mg/50 mL) (Mylan Pharm, St-Priest, France). A single dose of 7 mg/kg was given intraperitoneally (i.p.) (Ateşşahin, Karahan *et al.*, 2006, Ali, Hassanein *et al.*, 2021). Trypsin, DMEM, foetal bovine serum, collagenase type 1, penicillin-streptomycin, and phosphate-buffered saline (PBS), from (Sigma-Aldrich, St. Louis, USA) were obtained

3. Experimental Design:

The following four equal groupings of animals (n = 8) were created:

Group I: received a single injection of isotonic saline intraperitoneally (Control group).

Group II: was given the cisplatin intraperitoneally (i.p.) at a single dose of 7 mg/kg, and then they were left for five days later (Ateşşahin, Karahan *et al.* 2006, Ali, Hassanein *et al.* 2021) (Cisplatin-treated group).

Group III: was given the same dose of cisplatin, then after five days, they received a single injection of ADMSCs (1×10^6) mL intravenously into the tail vein (Ammar, Sequiera *et al.* 2015), and after that, the animals were left for 60 days more (Stem cell-treated group).

Group IV: was given cisplatin as previously reported and then left without intervention for 65 days (Withdrawal group).

4. Isolation and Transplantation of Mesenchymal Stem Cells:

Isolation of Mesenchymal Stem Cells:

Lipoaspirate (60-100 mL) was used to isolate MSCs obtained from liposuction procedures (Murphy and Atala 2013) at Assiut University's Plastic Surgery Department in Assiut, Egypt.

Isolation protocol was followed. Lipoaspirate was dispensed in

50 mL falcon tubes and washed with 1% antibiotic phosphate buffer saline (PBS). After that, it was digested using an equivalent volume of warm, filtered 0.1% collagenase type-1 solutions that were dissolved in PBS and heated to 37 °C for 60 minutes. The cell pellet fell to the bottom of the lipoaspirate after it had been centrifuged, and the fatty layer that had been floating in the supernatant was discarded. Reconstituted in full fresh medium, the cell pellet was then cultivated in 75 cm² culture flasks after being filtered through a 100 m nylon cell strainer (Falcon). After 48 hours, the media was changed in order to remove non-adherent cells by aspirating the old media, after every 2-3 days, then another change was made until confluence reached 80–90%.

5. Immunophenotyping Using Fluorescence-Activated Cell Sorting (FACS):

After passage two Stem cells were taken. Cultured cells were subjected to a 10% trypsin EDTA solution in the incubator for 5–10 minutes before being rinsed. Following this, the cell pellet was incubated for 1 hour with primary antibodies against CD90 and CD34 cell surface markers (Santa Cruz Biotechnology) and then for 30 minutes with the secondary antibody (Alexa flour 647). They were immunophenotyped utilizing a FACS flow cytometer after being washed twice. (Becton Dickinson, Heidelberg, Germany) (Meligy, Shigemura *et al.*, 2012).

6. Injection of Mesenchymal Stem Cells:

Using an insulin syringe, ADMSCs (1×10^6) suspension dissolved in PBS as a vehicle-injected into the tail vein recipient (stem-cell-treated group) (Ammar, Sequiera *et al.*, 2015).

7. RT-PCR Extraction:

To detect the HLA-B2704 gene, which identifies human stem cells, total RNA was extracted from the left ventricle of rat cardiac muscles. Major Histocompatibility Complex (MHC) proteins, which control the adaptive

immune system in humans, are encoded by the HLA locus (Jang, Choi *et al.*, 2019).

The RNA sample was dissolved in water devoid of RNase before being measured spectrophotometrically. RNA was extracted using Gene Zol™ CT RNA extraction reagent (Genetix Biotech Asia, Shivaji Marg, New Delhi, India). Then, RNA was reverse transcribed into cDNA using the High-Capacity cDNA Reverse Transcription

Kit (Applied Bio-systems Inc., CA, USA). To measure gene expression, SYBR Green Real-Time PCR Master Mix was utilized. The results were normalized against internal control genes known as housekeeping genes (GAPDH). The real-time PCR reaction outcomes were examined using Applied Biosystem Step OnePlus™ software using the Comparative Ct ($\Delta\Delta$ Ct) method (Livak and Schmittgen 2001).

Table 1: Primer's sequence.

	Forward	Reverse
GAPDH	GCATCTTCTTGTCAGTGCC	ACCAGCTTCCCATTCTCAGC
HLA-B2704	GCTACGTGGACGACACGCT	CTCGGTCAGTCTGTGCCT

8. Determination of Total Antioxidant Capacity (TAC) and Malondialdehyde (MDA) in Cardiac Tissue:

At the end of the experiment, cardiac tissues were homogenized in 10% ice-cold phosphate buffer saline (PBS). At 5000g for 15 minutes at 4°C, the homogenate was centrifuged. The supernatant was collected and stored at -20 °C for later analysis. Using commercially available colorimetric kits, TAC and MDA levels were determined (Bio-Diagnostics, Egypt). TAC was calorimetrically assessed using (Koracevic, Koracevic *et al.* 2001). The reaction of thiobarbituric acid with MDA produces a thiobarbituric acid reactive pink product, which is used to determine MDA. The total protein in the cardiac homogenate was measured and normalized using the Biuret reagent.

9. Determination of Tumor Nuclear Factor α (TNF- α) and Interleukin 2 (IL-2) in Cardiac Tissue:

According to the manufacturer's protocol and means of an enzyme-linked immunosorbent assay (ELISA) with rat specific TNF- α , and IL-2 levels in cardiac tissue homogenate were measured (Koma Biotech, Seoul, Korea) (MyBioSource, USA).

10. Histological Examination:

10.1. For Light Microscopy:

At the end of the experiment, the animals were anesthetized with an i.p. injection of thiopental sodium (50 mg/kg). The hearts of animals were exposed and perfused with saline until the blood flow was stopped. To complete the perfusion, 10% formalin was used. After perfusion, the hearts were dissected and fixed with 10% formalin, then sectioned into 2-mm-thick transverse slices from the cardiac muscles' left ventricles, embedded in paraffin, and cut into 4- μ m slices insert (Bancroft and Gamble 2008). H&E staining was applied for the sections, as well as immunohistochemical staining for the following antibodies.

- Caspase-3 (1:100 a rabbit polyclonal antibody, CPP32, Ab-4 IgG) antibody for detection of apoptotic cells purchased from Thermo Fisher Scientific; Fremont, USA.
- Proliferating cell nuclear antigen (PCNA) 0.1 ml at 200 micrograms (μ g)/ml concentrated 1ry Ab (PCNA Ab-1) (Labvision, USA).
- Vascular endothelial growth factor (VEGF) (1:100 a rabbit polyclonal Ab-1; IgG) to detect angiogenesis, purchased from Thermo Fisher Scientific; Fremont, USA.
- CD-105 antibody for detection of homed stem cells (1:100 a rabbit polyclonal Ab-1; IgG, purchased from Abcam-Boston, USA).

- e. CD-44 antibody (1:400 a mouse monoclonal antibody clone 2A4 for detection of homed stem cells (Nakagawa, Akita et al. 2005) purchased from Sigma-Aldrich, USA.

The immunohistochemical staining was done using the avidin-biotin-peroxidase complex technique. Five-millimeter paraffin-embedded sections were deparaffinized in xylene and rehydrated in alcohol. Sections were boiled for 15 minutes in a 10-um citrate buffer with a pH of 6.0 before cooling at room temperature for 20 minutes. Primary antibodies were added for one hour. According to the manufacturer's instructions, the sections were processed using the universal kit (EcnTek HRP Anti-Polyvalent, DAB) (ScyTek Laboratories, Inc. 205 South 600 West Logan, UT84321, USA). After the reaction was finished, Mayer's Hematoxylin was used for counterstaining, and it was then dehydrated, and cover-slipped with DPX.

10.2. For Electron Microscope:

Through two transverse cuts made at one-third and two-thirds of the left ventricle's length, cardiac tissues were retrieved as full-thickness slices of the wall (Meligy, El-Deen Mohammed et al. 2022). This midventricular slice was fixed for 4 hours at 4 degrees Celsius in 4% glutaraldehyde. From glutaraldehyde-fixed specimens, semithin sections (0.5–1 m thick) were prepared and stained with toluidine blue. In the Electron Microscope Unit at Assiut University, ultrathin sections (500-800°) were cut from selected semithin sections, contrasted with uranyl acetate and lead citrate (Glauert and Lewis 2014), studied with a JEOL transmission electron microscope (JEM-100CXII; Akishima, Tokyo, Japan), and photographed at 80 kV.

10.3. Morphometric Study:

The area % of the anti-caspase 3 +ve immunoexpression at (x400 magnification) was estimated by the open-resource image software Image J.

Five serial sections of the cardiac myocytes of 3 rats from each group were randomly selected.

Measurement of the number of PCNA-positive nuclei of cardiac myocytes and VEGF-positive capillaries was performed in random immune-stained 10 high power (x400) non-overlapping fields for each section from 3 rats in each group. At the Histology Department, Faculty of Medicine, Assiut University, computerized image analyzer system software (LeicaQ 500 MCO, Leica) and a camera attached to a Leica universal microscope was used.

10.4. Statistical Analysis:

The data were presented as mean \pm standard deviation (mean \pm SD). The one-way analysis of variance (ANOVA) test with post-hoc analysis was used to assess the significance of differences between the means. It was done with the help of the SPSS program, version 20 (Inc., Chicago, USA). At $P \leq 0.05$ were considered significant,

RESULTS

1. Flow Cytometric Analysis of ADMSCs:

The ADMSCs declared a strong expression of the CD90 marker, but a very weak expression of CD34 (Fig. 1a).

2. Microscopic Morphology of ADMSCs:

Phase contrast microscopy examination of ADMSCs revealed rounded isolated cells of varying sizes, the majority of which floated on the surface of the newly cultured cells. A few cultured cells had attached to the plate after one day, forming an elongated spindle with long cytoplasmic processes. After 7 days, the confluent state reached about 80%, and the field was crowded and connected forming a whorl appearance (Fig.1b).

3. RT-PCR Gene Expression:

After normalization with the housekeeping gene GAPDH, the gene expression of HLA-B2704 in our study was highest in the stem cell-treated group which indicated homing of human mesenchymal stem cells to the cardiac tissue (Fig.1c).

4. Effect on TAC, MDA, TNF- α , and IL-2 Levels in Cardiac Tissue:

The level of TAC in the cardiac tissue of the cisplatin-treated group revealed a significant decrease versus the control group ($P < 0.0001$). Treatment with stem cells improved the level of TAC significantly if it is compared with the cisplatin-treated group ($P < 0.0001$). Although improvement occurred in the levels of TAC in the stem cell-treated group, their levels were still significantly lower than that of the control group ($P < 0.001$). The withdrawal group showed a significant decrease in the level of TAC versus both the control ($P < 0.0001$) and stem cells-treated ($P < 0.05$) groups. In comparison with the cisplatin-treated group, the withdrawal group revealed a significantly increased level of TAC ($P < 0.05$) (Table 1).

The levels of MDA were significantly higher in the cardiac tissue of the cisplatin-treated group than in the control group ($P < 0.0001$). A significant reduction in the level of MDA was noticed in rats treated with stem cells when compared with the Cisplatin-treated group ($P < 0.0001$) but still significantly more than the control group ($P < 0.0001$). MDA levels in rats in the

withdrawal group were significantly more than their levels in rats in the control group ($P < 0.0001$) and the stem cells-treated group ($P < 0.05$). When compared against the Cisplatin-treated group, the levels of MDA in the withdrawal group were significantly lower ($P < 0.05$) (Table1).

The significantly increased levels of TNF- α and IL-2 in the cardiac tissue of the cisplatin-treated group were noticed versus the control group ($P < 0.0001$ and $P < 0.0001$; respectively). Treatment with stem cells resulted in a significant reduction in the levels of TNF- α and IL-2 in comparison with the cisplatin-treated group ($P < 0.001$ and $P < 0.0001$; respectively). Still, the levels of TNF- α and IL-2 in the stem cells-treated group were more than the control group ($P < 0.05$ and $P < 0.05$; respectively). The withdrawal group revealed significantly higher levels of TNF- α and IL-2 than the control group ($P < 0.0001$ and $P < 0.0001$; respectively) and the stem cells-treated group ($P < 0.05$ and $P < 0.01$; respectively). Insignificant differences in the levels of TNF- α and IL-2 in the withdrawal group were obtained in comparison with the Cisplatin-treated group (Table1).

Table 1: Levels of total antioxidant capacity (TAC), malondialdehyde (MDA), TNF- α , and IL-2 in the cardiac tissue of different groups.

	Control Group	Cisplatin-treated group	Stem cells - treated group	Withdrawal group
TAC ($\mu\text{mol}/\text{mg}$ protein)	0.42 \pm 0.09	0.09 \pm 0.01 ^a	0.27 \pm 0.02 ^{a, b}	0.17 \pm 0.01 ^{a, b, c}
MDA (nmol/ mg protein)	1.10 \pm 0.20	2.74 \pm 0.33 ^a	1.93 \pm 0.18 ^{a, b}	2.35 \pm 0.15 ^{a, b, c}
TNF- α (ng/mg protein)	0.48 \pm 0.08	0.76 \pm 0.07 ^a	0.59 \pm 0.04 ^{a, b}	0.73 \pm 0.03 ^{a, c}
IL-2 (pg/mg protein)	10.04 \pm 2.19	19.43 \pm 1.98 ^a	13.41 \pm 1.46 ^{a, b}	17.39 \pm 0.75 ^{a, c}

Data are presented as means \pm SD. ^a Significant when compared to the control group. ^b Significant when compared to the cisplatin-treated group. ^c Significant when compared versus stem cells-treated group. $p \leq 0.05$

5. Histological and Immunohistochemical Results:

5.1. Light microscopy results:

Hematoxylin and eosin-stained sections of the control cardiac myocytes showed a regular arrangement of the muscle fibers. The muscle fibers appeared branching anastomosing, and the cardiomyocytes declared striated

acidophilic cytoplasm studded with myofibrils and oval central vesicular nuclei. (Fig. 2a).

The Cisplatin-treated group revealed severe disorganization of the architecture of muscle fibers that showed focal lysis and widening of the spaces among the myofibrils with areas of complete loss of the myofibrils.

Most of these myofibrils appeared swollen. The nuclei appeared markedly distorted and highly condensed. congestion and dilation of blood capillaries between cardiac fibers were also observed (Fig.2b).

In Stem cell-treated group, the cardiac myocytes showed the nearly normal histological structure of most cardiac fibers. The myofibrils were regularly organized. Cardiac muscle fibers appeared branching, cylindrical and anastomosing, and most of them exhibited central oval vesicular nuclei. Very few muscle fibers revealed pale cytoplasm and some swollen myofibrils (Fig. 2c).

The Withdrawal group revealed few muscle fibers relatively restoring the normal appearance, while other fibers still declared intensive disruption with the appearance of multiple vacuoles within the sarcoplasm and the appearance of abundant spaces among the myofibrils. The nuclei of some fibers appeared irregular, deeply stained, and pyknotic with noticeable distortion of the nuclear appearance. In the intercellular spaces, the blood capillaries were dilated and congested with an area of extravasated blood (Fig. 2d).

5.2 Immunohistochemistry:

Examination of caspase3-immunostained sections revealed slight immunoreactivity in some cardiac myocytes of the control group (Fig. 3a). A strongly positive reaction could be observed in some cardiac myocytes of the cisplatin-treated group (Fig.3b). After MSCs administration, there was an evident decrease in caspase3 immunoreactivity in cardiac muscle fibers (Fig. 3c). In withdrawal group, a decrease in the caspase3-immunostained cardiac myocytes was noticed (Fig. 3d) in comparison to the cisplatin-treated group, but still higher than control and stem cell-treated groups.

Proliferating cell nuclear antigen (PCNA)-immunostained sections of the control cardiac muscle showed multiple positive nuclei among

cardiac myocytes (Fig. 4a). Few PCNA-positive nuclei were observed among cardiac myocytes of the cisplatin-treated group (Fig. 4b). Multiple immunopositive nuclei were observed among cardiac myocytes of MSCs-treated group (Fig.4c). The presence of few PCNA positive nuclei was observed among myocytes of withdrawal group (Fig.4d).

VEGF-immunostained sections revealed a normal distribution of positive immunostained endothelial cells lining the wall of blood vessels among the cardiac myocytes of the control group (Fig. 5a). Multiple positive immunostained endothelial cells were seen in the wall of blood vessels of the cisplatin-treated group (Fig. 5b). Obvious numerous VEGF immunostained cells could be seen in the wall of blood vessels among the cardiac myocytes of MSCs treated group (Fig. 5c). Nearly normal distribution of positive immunostained cells was observed in the wall of the blood vessels of the withdrawal group (Fig. 5d).

Examination of CD105-immunostained sections revealed negative reactions in the control, cisplatin-treated, and withdrawal groups (Figs. 6a, 6b, 6d). On the other hand, multiple positive immunostained cells could be observed among the cardiac myocytes of the ADMSCs treated group (fig. 6c).

Examination of CD44-immunostained sections showed negative reactions in the control, cisplatin-treated, and withdrawal groups (Figs. 7a, 7b, 7d). Multiple positive immunostained spindle-shaped cells were detected among the cardiac myocytes of the ADMSCs treated group (fig. 7c).

5.3. Electron Microscopic Examination:

Ultrastructural examination of the myocardium of the control groups revealed that the cardiac muscle cells have intact sarcolemma with long parallel arrays of myofibrils and well-defined sarcomeres. Their nuclei were

centrally located and oval, surrounded by an intact nuclear membrane with finely dispersed chromatin. The mitochondria were abundant, elongated or spherical in shape, and regularly arranged in rows in between the myofibrils. Each mitochondrion contained closely packed cristae (Fig. 8a). Also, regular striation between Z-lines with the dark A-band in the middle and the light I-band in the periphery was observed. A light H-zone was also noticed in the center of the dark A-band. The myofibrils were closely adherent to each other. (Fig.9a).

Electron microscopic study of the Cisplatin-treated group revealed remarkably disorganized, fragmented attenuated myofibrils with loss of cross striations. The mitochondria appeared irregularly arranged, varying in size and shape, some appeared shrunken disfigured, and others appeared swollen with the destruction of the cristae. The nucleus revealed irregularity in shape with infoldings of the outer membrane with an abnormal pattern of nuclear chromatin (Fig. 8b). Undulating irregular sarcolemma of the cardiac myocytes, and wide spaces were seen around the nucleus and in the sarcoplasm (Figs. 8c). Noticeable wide separation among the degenerated myofibrils was seen with the appearance of multiple vacuoles. These changes lead to the disarrangement and disorganization of Z-lines and H-zones (Fig. 9b).

In animals treated with stem cells, the ultrathin section revealed an almost normal appearance of cardiac muscle fibers. The mitochondria were mostly more arranged and re-organized in between myofibrils compared with the previous groups. However, still some appeared swollen with destructed cristae and destructed outer membranes. Some nuclei still declared irregular outlines and clumps of heterochromatin specially condensed on the outer membrane (Fig. 8d). The myofibrils appeared organized with the ordinary structure of sarcomere with well-defined two Z lines, dark (A) and light (I) bands. The narrow

intercellular spaces with close apposition of the sarcolemma of adjacent fibers were observed (Fig. 9c).

The withdrawal group revealed some loss of the ordinary organization of the sarcomere with vacuolated areas within the sarcoplasm. The mitochondria displayed various degrees of degeneration and loss of normal arrangement. They appeared dense and pleomorphic in shape. Some appeared swollen and showed partial loss of cristae. Others appeared condensed and shrunken. The nucleus with abnormal faint chromatin distribution was observed (Fig.8e). Disorganization of myofibrils associated with disarrangement of Z lines and the content of sarcomere were observed (Fig. 9d).

5.4. Morphometric Assessment of Immunohistochemical Results:

The percentage area fraction of caspase-3 indicated a significant increase in the cisplatin-treated group in comparison with the control group ($P < 0.0001$). Utilizing stem cell treatment succeeded in a significant reduction in the percentage area fraction of caspase-3 when compared with the cisplatin-treated group ($P < 0.001$). However, still, the percentage area fraction of caspase-3 in the stem cell-treated group was significantly higher than the control group ($P < 0.01$). The withdrawal group showed a significant increase in the percentage area fraction of caspase-3 versus both the control ($P < 0.0001$) and the stem cell-treated ($P < 0.05$) groups but revealed a significant decrease versus the cisplatin-treated group ($P < 0.05$) (Table 2 & Fig. 3).

The number of PCNA immunoreactive cells /field was significantly reduced in the cisplatin-treated group in comparison with the control group ($P < 0.0001$). Treatment with stem cells resulted in a significantly increased number of PCNA immunoreactive cells /field when compared with the cisplatin-treated ($P < 0.0001$), and the control group ($P < 0.001$) groups. A significant reduction in

the number of PCNA immunoreactive cells /field was noticed in the withdrawal group versus both the control group ($P < 0.0001$) and the stem cell-treated ($P < 0.0001$). A non-significant difference was obtained when comparing the withdrawal group versus the cisplatin-treated group ($P > 0.05$). (Table 2 & Fig. 4)

The number of VEGF immunoreactive cells /field was significantly increased in the cisplatin-treated group in comparison with the control group ($P < 0.0001$). Rats treated

with stem cells showed a significant increase in the number of VEGF immunoreactive cells /field in comparison with the cisplatin-treated ($P < 0.0001$) and the control group ($P < 0.0001$) groups. The withdrawal group showed a significantly higher number of VEGF immunoreactive cells /field than the control group ($P < 0.001$) and a significantly lower number than the stem cells-treated group ($P < 0.001$) while, a non-significant difference against the cisplatin-treated group ($P > 0.05$) (Table 2 & Fig.5).

Table 2: Statistical analysis of % area of caspase intensity, PCNA, and VEGF immunoreactive cells per field in cardiac myocytes in all groups studied.

	Control Group	Cisplatin-treated group	Stem cells - treated group	Withdrawal group
% Area fraction of caspase 3	16.93 ± 1.27	49.92 ± 5.89 ^a	30.12 ± 1.39 ^{a, b}	39.77 ± 1.06 ^{a, b, c}
Number of PCNA immunoreactive cells /field	9.17 ± 0.75	2.20 ± 0.45 ^a	12.17 ± 1.47 ^{a, b}	3.17 ± 0.75 ^{a, c}
Number of VEGF immunoreactive cells /field	2.33 ± 0.52	4.33 ± 0.51 ^a	7.33 ± 0.52 ^{a, b}	4.00 ± 0.63 ^{a, c}

Data are presented as means ± SD. ^a Significant when compared to the control group. ^b Significant when compared to the cisplatin-treated group. ^c Significant when compared versus stem cells-treated group. $p \leq 0.05$.

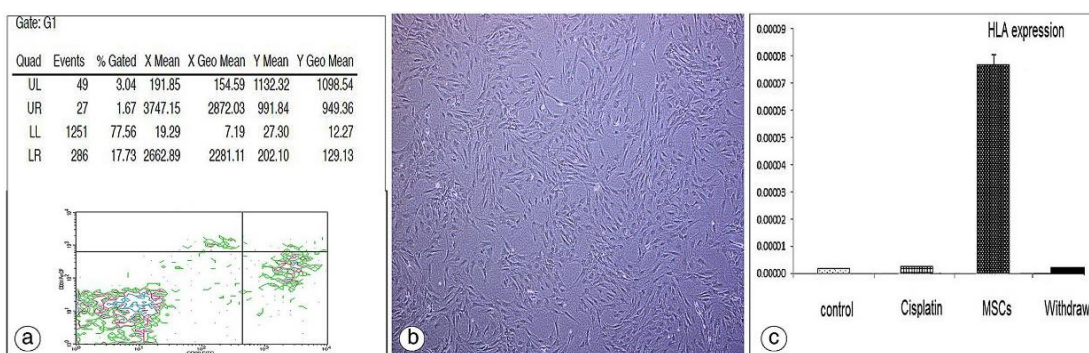


Fig. 1: (a) FACS analysis of isolated stem cells showed that the adipose-derived MSC were negative for CD34 markers but strongly positive for CD90. (b) A phase-contrast micrograph showing cultured mesenchymal stem cells with a fibroblast-like shape and fusiform nucleus ($\times 200$). (c) RT -PCR gene expression showing highest expression of HLA-B2704 in the stem cell treated group.

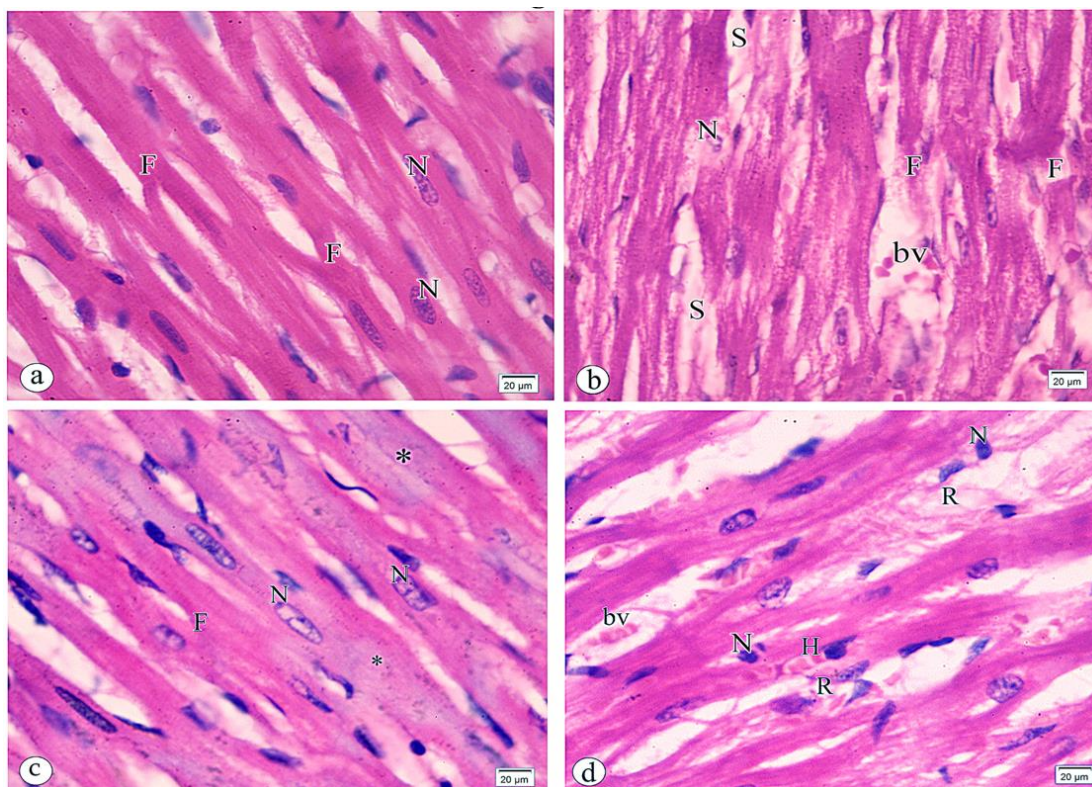


Fig. 2: photomicrographs of H&E-stained longitudinal sections of the cardiac muscle, (a) Control group showing branching, anastomosing and striated cardiac muscle fibers (F). Central oval vesicular nuclei (N) and acidophilic sarcoplasm can be noticed, scale bar = 20 µm. (b) Cisplatin treated group showed extensively disrupted organization of muscle fibers that appeared remarkably damaged with focal lysis (F) with a widening of the spaces among the myofibrils (S)). severely distorted nuclei (N) which appeared highly condensed and had irregular malformed shapes were declared. The congested dilated blood vessel can be also observed (bv), scale bar = 20 µm. (c) MSCs treated group showing the apparently normal microscopic structure of the cardiac myocytes with branching and syncytial arrangement of myofibrils (F) with central vesicular nuclei (N). Notice the appearance of some muscle fibers with pale cytoplasm and very few swollen myofibrils (*) (scale bar =20 µm). (d) Withdrawal group showing relatively some muscle fibers begin to restore to normal appearance (F). Congested dilated blood vessels (bv), an area of extravasated blood or hemorrhage (H), and some deeply stained highly condensed nuclei (N) were noticed (scale bar = 20 µm).

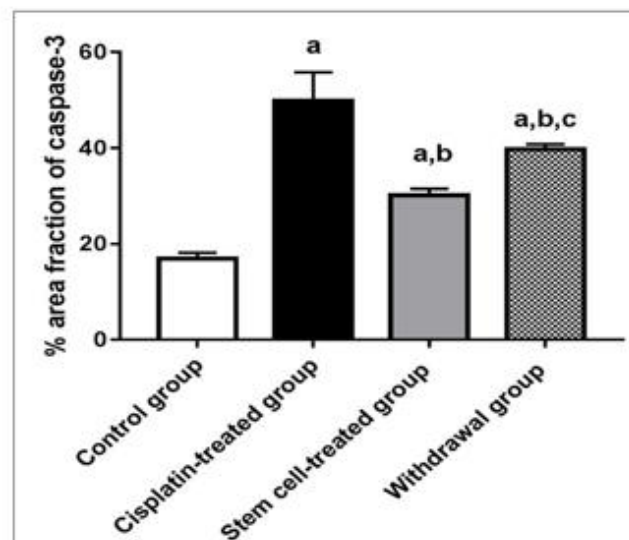
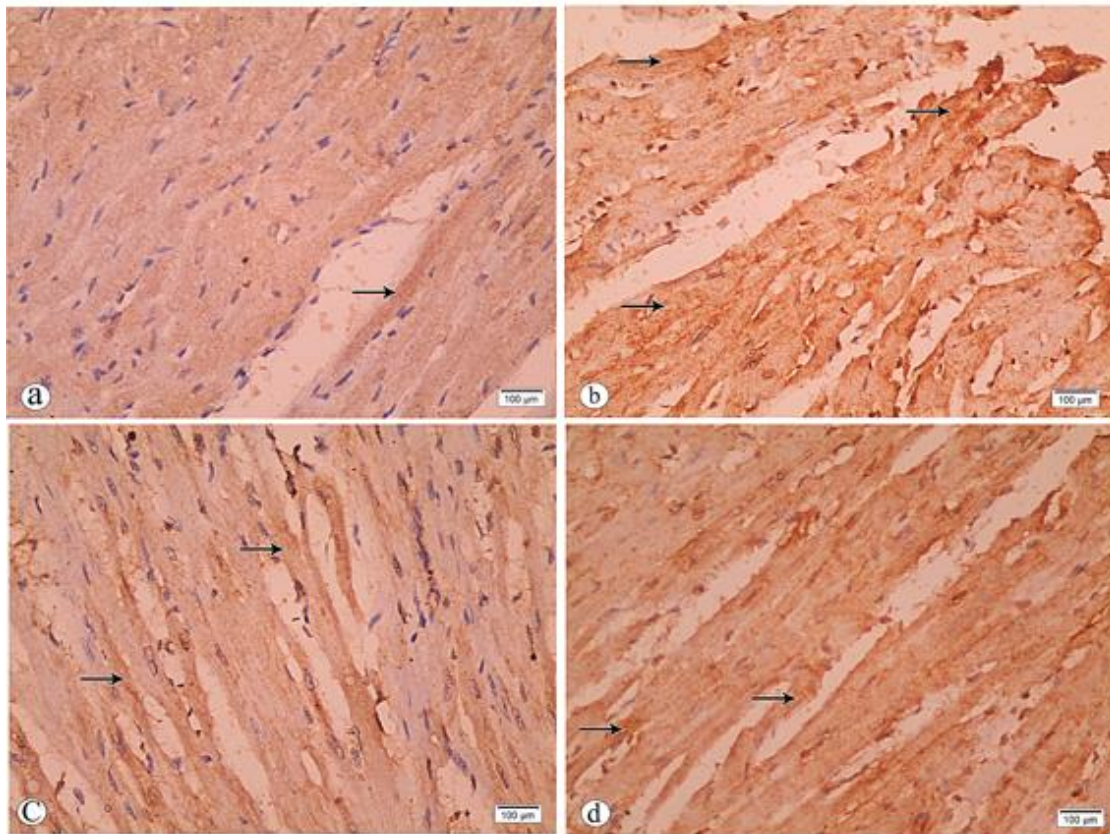


Fig.3: Photomicrographs of caspase3 immunostained sections of cardiac muscles, (a) Control group showing slight immunoreactivity in some cardiac fibers (↑). (b) Cisplatin treated group showing strong immunoreactivity in some cardiac fibers (↑). (c) MSCs treated group showing moderate immunoreactivity in few cardiac fibers (↑). (d) Withdrawal group showing strong immunoreactivity in few cardiac fibers (↑). (scale bar =100 um).

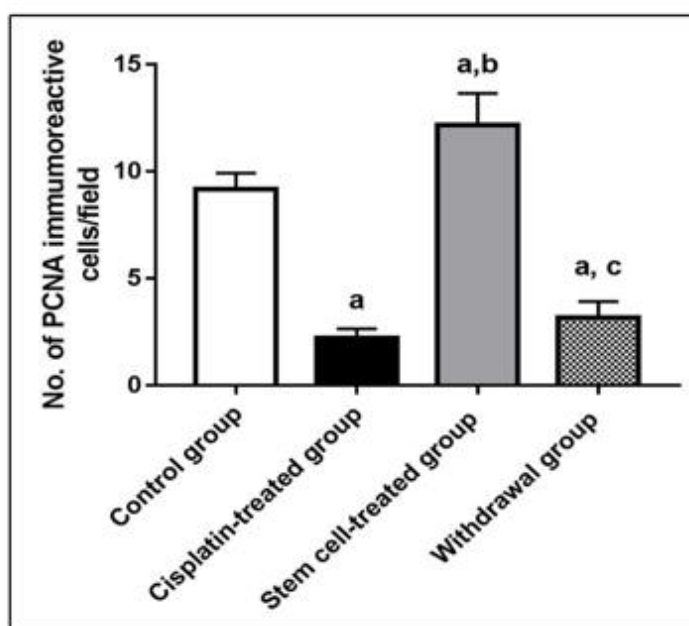
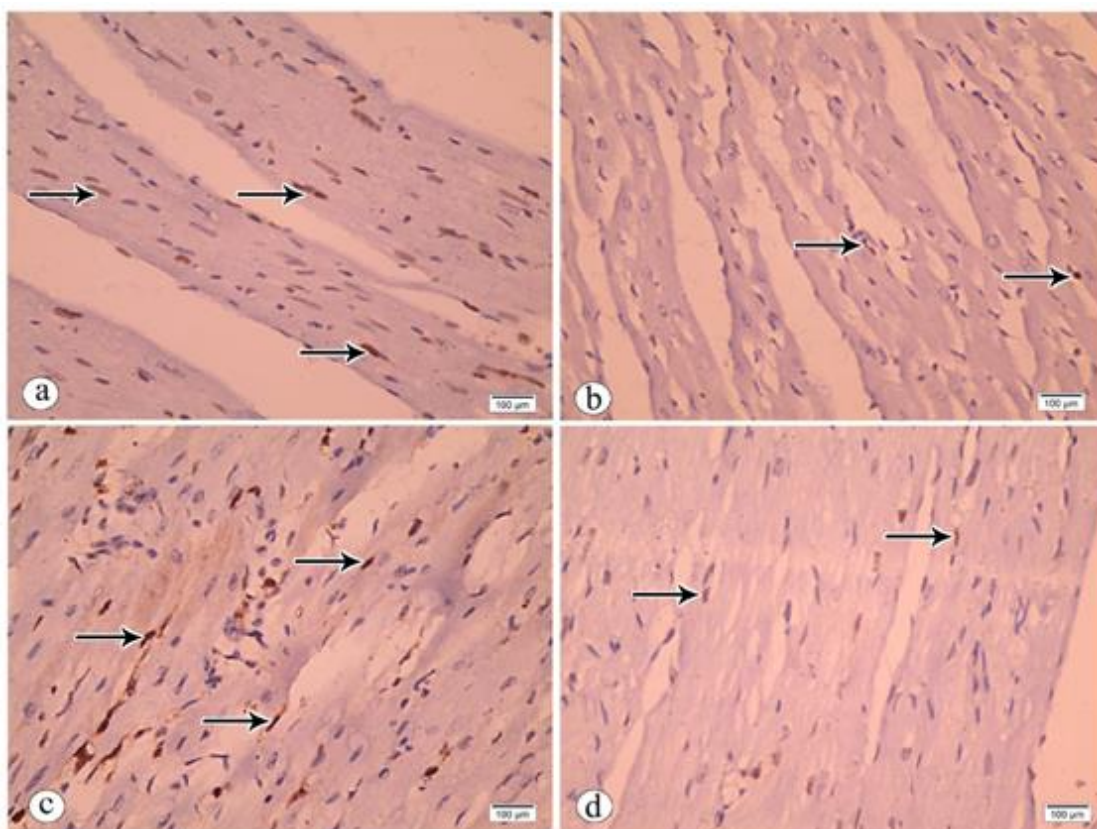


Fig. 4: Photomicrographs of PCNA immunostained sections of cardiac muscle fibers. (a) Control group showing multiple immunoreactive positive nuclei among cardiac myocytes (↑). (b) Cisplatin treated group showing few immunoreactive positive nuclei among cardiac myocytes (↑). (c) MSCs treated group showing multiple immunoreactive positive nuclei among cardiac myocytes (↑). (d) Withdrawal group showing few immunoreactive positive nuclei among cardiac myocytes (↑). (scale bar =100 um).

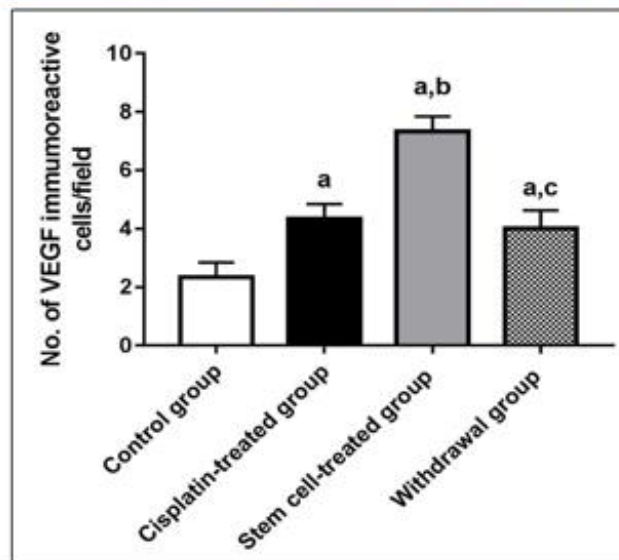
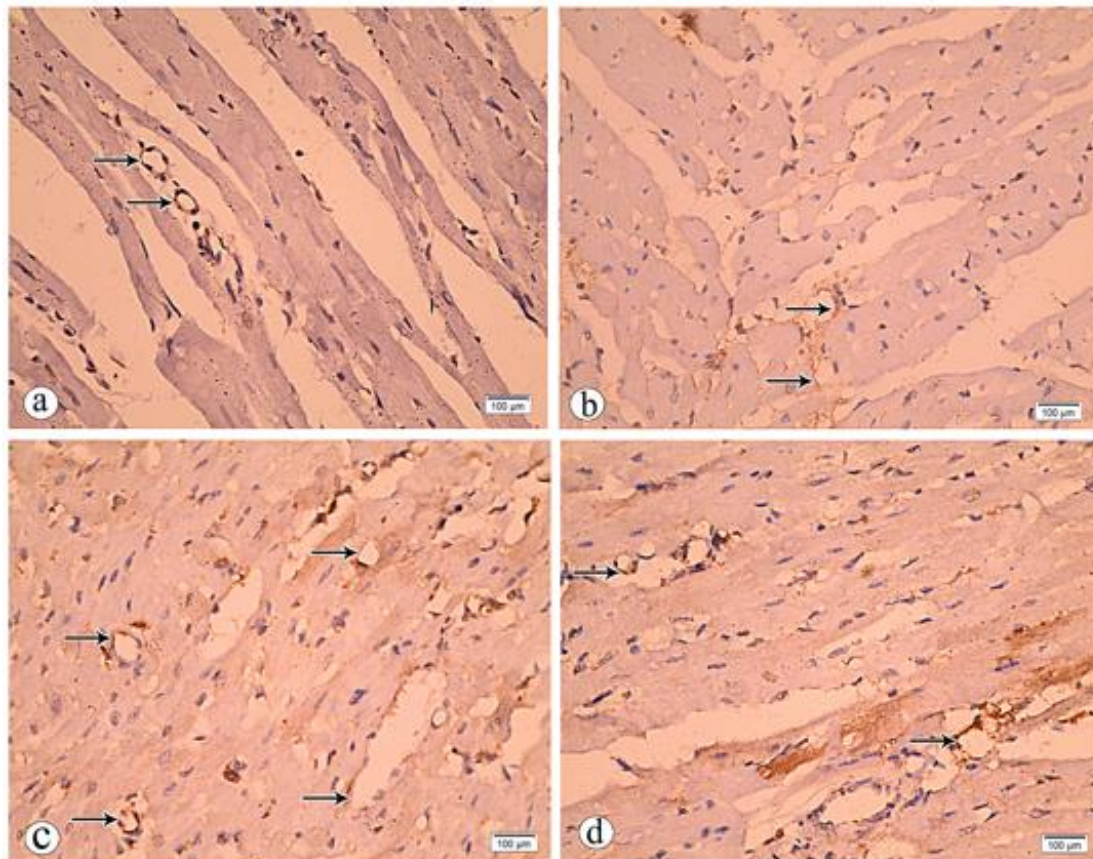


Fig.5: Photomicrographs of VEGF immunostained sections of cardiac muscle (a)Control group showing normal distribution of positive immunoreactive lining cells of blood vessels (↑). (b) Cisplatin treated group showing multiple positive immunoreactive lining cells of blood vessels (↑). (c) MSCs treated group showing obvious numerous positive immunoreactive lining cells of blood vessels (↑).(d) Withdrawal group showing nearly normal immunoreactive lining cells of blood vessels (↑).(scale bar =100 μm).

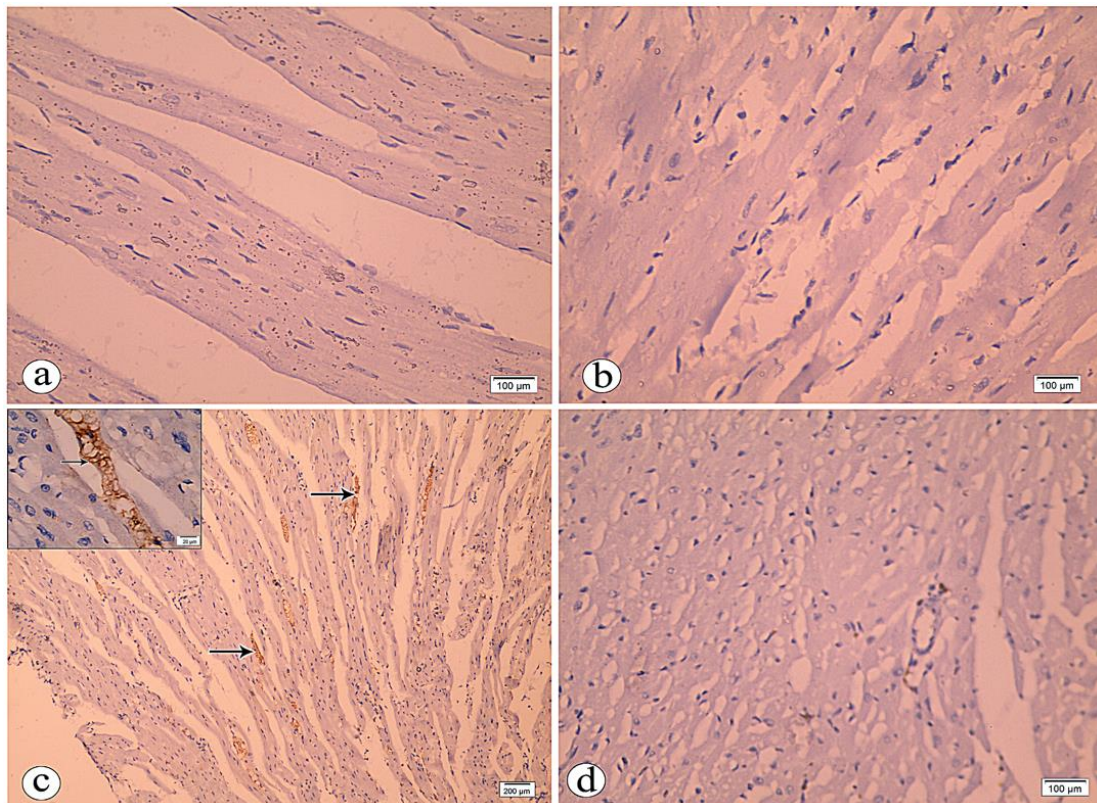


Fig. 6: Photomicrographs of CD 105 immunostained sections of cardiac muscle (a) Control group showing negative immunoreactivity among the cardiac myocytes (scale bar =100 um).(b) Cisplatin treated group showing negative immunoreactivity among the cardiac myocytes (scale bar =100 um). (c) MSCs treated group showing multiple immunoreactive positive cells among the cardiac myocytes (↑) (scale bar =200 um). (d) Inset: Higher magnification of the previous section showing immunoreactive positive MSCs cell (↑) (scale bar = 20 um). (e) Withdrawal group showing negative immunoreactivity among the cardiac myocytes. (Scale bar =100 um).

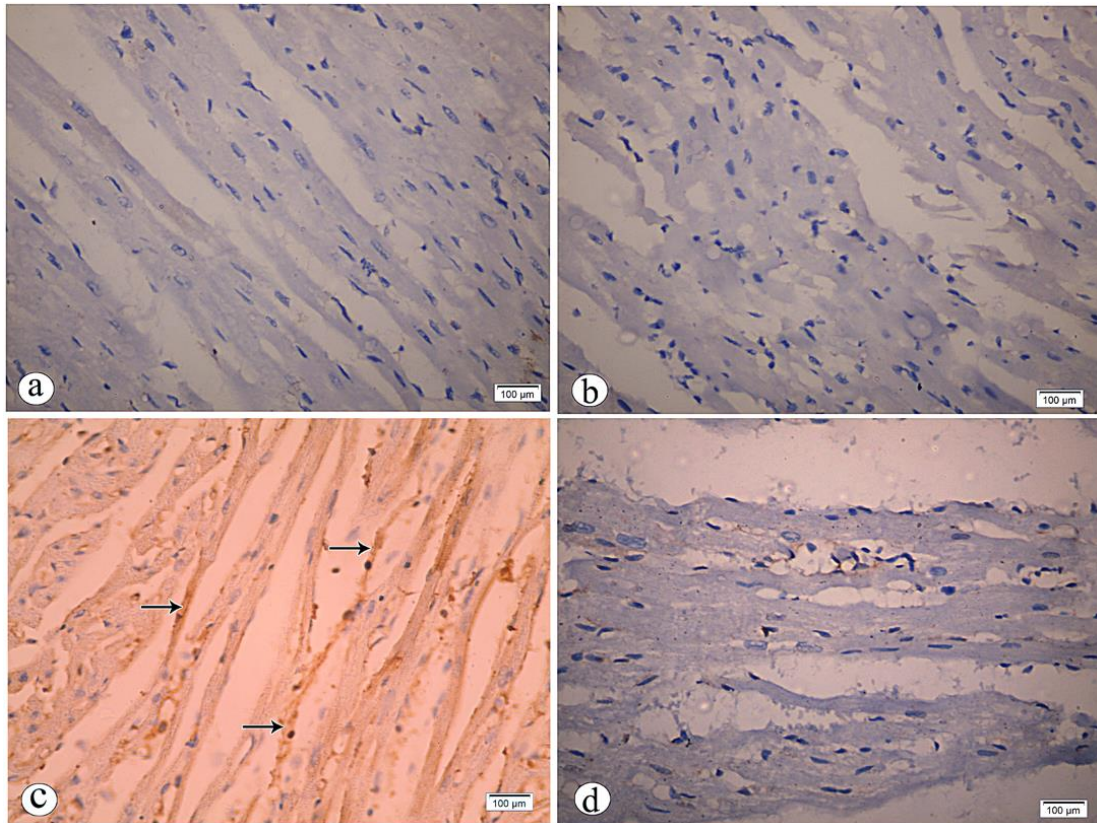


Fig. 7: Photomicrographs of CD 44 immunostained sections of cardiac muscles. (a) Control group showing negative immunoreactivity among the cardiac myocytes. (b) Cisplatin-treated cardiac muscle showing negative immunoreactivity among the cardiac myocytes. (c) MSCs treated group showing multiple immunoreactive positive cells among the cardiac myocytes (↑). (d) Withdrawal group showing negative immunoreactivity among the cardiac myocytes. (Scale bar =100 um).

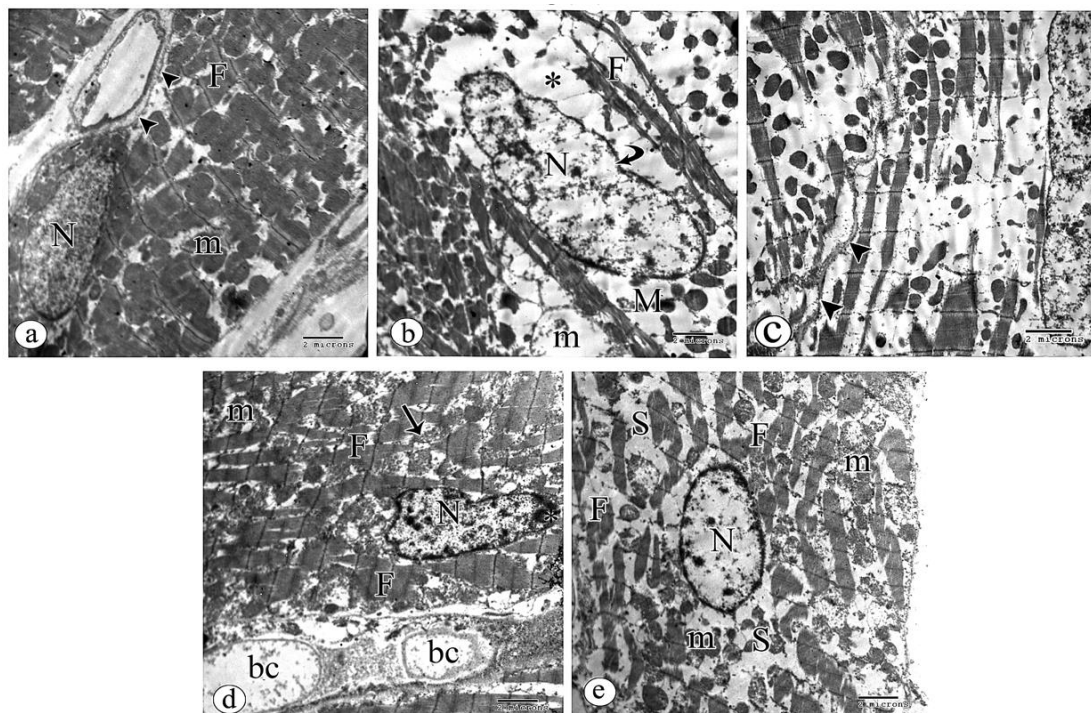


Fig. 8: Electron-micrographs of sections from rat heart. (a) Control group showing cardiac muscle cells had regular sarcolemma (arrowheads), long parallel arrays of myofibrils (F) with an oval euchromatic nucleus (N), and dispersed chromatin. Rows of mitochondria (m) are observed among cardiac muscles. (b) Cisplatin-treated group showing disorganized, fragmented myofibrils (F). Irregularly arranged mitochondria, some appeared shrunken disfigured (M), and others appeared swollen with the destruction of the cristae (m). The nucleus (N) revealed irregularity of the outer membrane (curved arrow) with an abnormal appearance of the chromatin pattern. Notice the wide spaces (*) around the nucleus and in the sarcoplasm of the cardiac myocytes. (c) Cisplatin treated group showed undulating irregular sarcolemma (arrowheads). (d) MSCs treated group showing a nearly regular arrangement of the myofibrils (F). Mitochondria (m) displayed to a great extent normal arrangement, however, still some are showing destroyed cristae (arrow). The nucleus (N) declared an irregular outline and clumps of heterochromatin specially condensed on the outer membrane (*). Note: Appearance of blood capillaries (bc). (e) Withdrawal group reveals the degenerated disrupted myofibrils (F). The mitochondria (m) appeared shrunken with the loss of their cristae. The nucleus (N) shows abnormal faint chromatin distribution. Note the numerous wide spaces (S) among myofibrils. (TEM, X 4800).

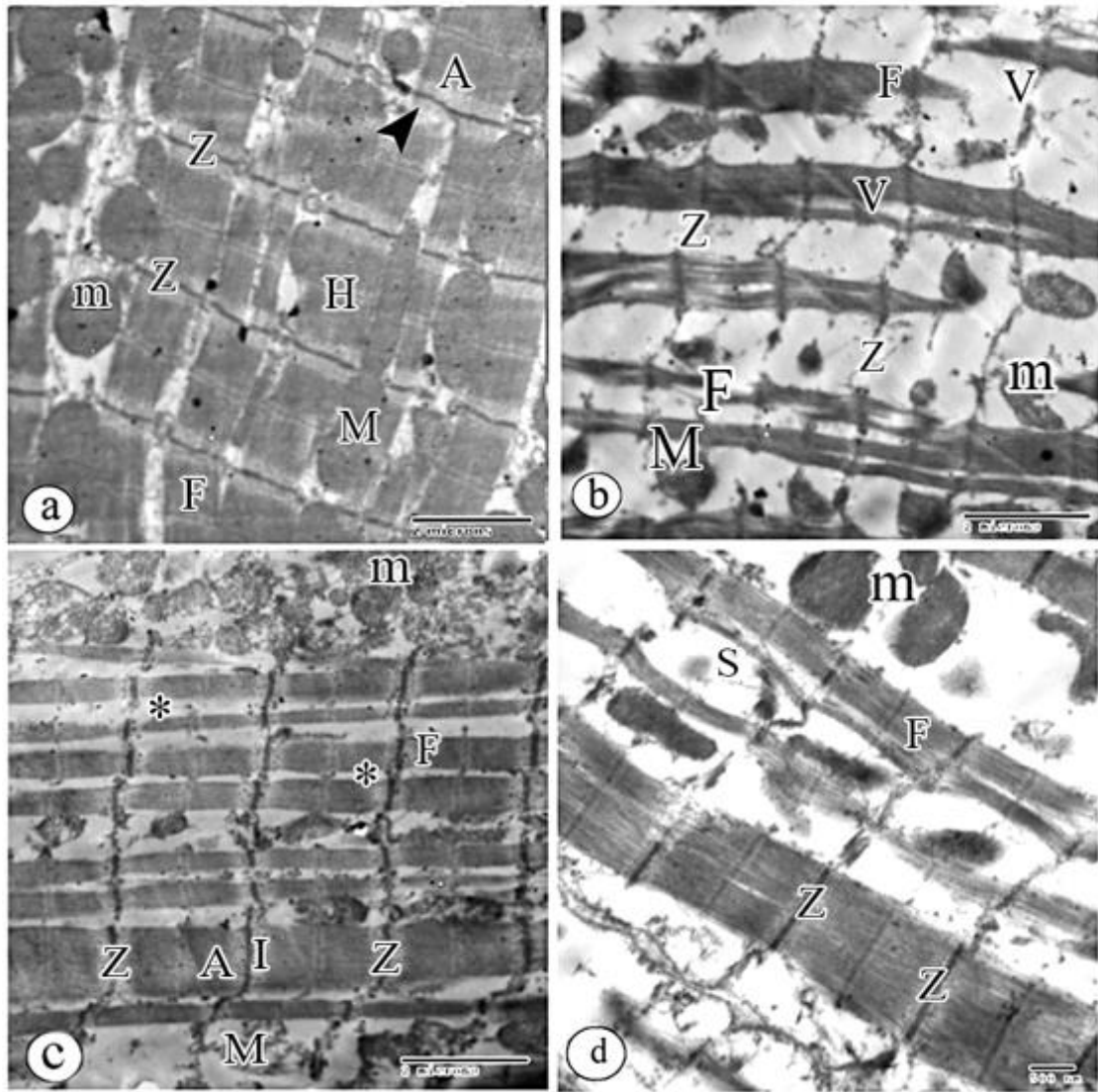


Fig. 9: Electron micrographs of sections from rat heart, (a) Control group showing regular transverse striations of myofibrils (F) formed of alternating dark A bands (A) and light I bands (arrowhead) with regular Z lines (Z) in the middle of light bands. A light H-zone (H) could also be seen in the center of the dark A-band. Rows of spherical (m) and elongated (M) mitochondria are seen between myofibrils. (b) Cisplatin treated group showed remarkable separation of myofibrils that revealed multiple vacuoles (V) and myofibrillar fragmentation and degeneration (F). Notice the scanty mitochondria that appeared disorganized highly condensed (M) or with a ruptured membrane (m). (c) MSCs treated group showing great restoration to normal appearance. The myofibrils appeared organized (F) with an ordinary structure of sarcomere and well-defined two Z lines (Z), dark (A), and light bands (I). Mitochondria (m) appeared to retain normal arrangement. However, still some appeared swollen with destructed cristae (M) and destructed outer membrane Note: The narrow intercellular spaces with close apposition of the sarcolemma of adjacent fibers (*). (TEM, X10000) (d) Withdrawal group shows the myofibrils restore to some extent normal appearance (F) with well-defined Z lines in most areas (Z). Notice the wide spaces (S) among muscle fibers that revealed very few degenerated disruptive highly condensed mitochondria (m). (TEM, X14000).

DISCUSSION

The current study examined the influence of a single intraperitoneal injection of cisplatin on the histological structure of the cardiac muscle. In addition, we evaluated the possible role of adipose tissue mesenchymal stem cell therapy on the cisplatin-induced deterioration of cardiac injury and its pathophysiological pathways. Cisplatin treated group revealed extensively disrupted organization of muscle fibers that appeared remarkably damaged with focal lysis with the widening of the spaces among the myofibrils. severely distorted nuclei which appeared highly condensed and had irregular malformed shapes were also declared. Similar degenerative changes in the cardiac muscle were obtained by (Topal, Bilgin *et al.* 2018, Ibrahim, Bakhaat *et al.*, 2019). Cardiac lesions could be explained based on the oxidative stress increase in cardiac tissue evidenced by the decreased activities of the total antioxidant defense and the increased MDA levels in this study. MDA is considered an indicator of the degree of oxidative damage (Hideg and Kálai 2007). The damage to cardiac tissue could be due to the reaction of the generated radicals with the lipids and proteins of the cell membrane followed by damage of the nucleic acid with the release of cardiac enzymes (Conklin and Nicolson 2008). Other authors (Jomova and Valko 2011) explained those degenerative changes in the cardiac muscle based on decreased aerobic respiration and the reduction in ATP production due to mitochondrial damage, which is evident in this current study.

In this study, it was noticed that the levels of proinflammatory cytokines e.g., TNF- α and IL-2 were increased in the cardiac tissue of rats that received cisplatin which enhanced free radical formation. Moreover, cisplatin increased the nuclear factor kappa B (NF- κ B) expression, resulting in the subsequent formation of previously reported

proinflammatory cytokines (Francescato, Costa *et al.*, 2007). In addition, the reactive radicals changed the mitochondrial permeability with the subsequent release of cytochrome C and activated the mitochondrial pathway of apoptosis (Kim, He *et al.*, 2003, Qian, Nishikawa *et al.* 2005). Accumulating cisplatin within the cytoplasm of the myocytes with numerous mitochondria leads to mitochondrial DNA damage. The significant increase in the area percentage of caspase-3 immunoexpression in cardiac tissue denotes DNA damage due to cisplatin accumulation. This finding is inconsistent with what was reported by (El-Sawalhi and Ahmed 2014).

On the other hand, PCNA immunoexpression, the marker indicating nuclear activation, which is considered a crucial factor in DNA replication and repair pathways, and plays an essential role in genome stability, was investigated to determine the underlying molecular mechanisms of the effect of cisplatin and the protective effect of ADMSC. In the current work, the significantly fewer PCNA immune-stained cells in the cisplatin-treated group compared to those in the control indicated reduced proliferative activity in the former. On the other hand, the present findings showed that PCNA expression significantly increased in ADMSC-treated groups. PCNA contributes to ADMSC proliferation and resistance to apoptosis. Similarly, (Chen, Wang *et al.*, 2015 & Meligy, El-Deen Mohammed *et al.*, 2022) reported a decreased expression of PCNA-positive nuclei in the degenerated myocardium, which was accompanied by an increased caspase-3 in a reciprocal relationship.

The presence of PCNA immunopositive cardiomyocytes in the heart of control rats could be explained in view of what was reported by (Johnson, Mohsin *et al.*, 2021) who highlighted cardiomyocyte proliferation as a source of new myocyte development in the adult heart through manipulations

of the cardiomyocyte cell cycle, signaling pathways, endogenous genes, and environmental factors.

At the level of E.M in the present work, disruption, and lysis of myofibrils, mitochondria cristae damage, nuclear chromatin disintegration, and sarcoplasm vacuolation were observed. Such changes could be attributed to oxidative stress injury, mainly to cytoskeletal proteins. These effects agree with what is reported by Bukhari, Mohamed *et al.* (2022).

Similar results were obtained by other cytotoxic drugs on the myocardium as cyclophosphamide (Refaie, El-Hussieny *et al.* 2022) or doxorubicin (Pınarlı, Turan *et al.* 2013, Huang, Lei *et al.*, 2022) due to the toxic effects of these drugs in addition to the associated myocardial ischemia that leads to chromosomal aberrations, cardiac cell death, and apoptosis.

The present result revealed the presence of sarcoplasm vacuolation, which could be explained by the impairment of Na⁺-K⁺ pump mechanism based on observed mitochondrial cristae damage that may result in a drop in ATP levels, causing an influx of Na⁺ and H₂O. This will result in cell expansion and subsequent sarcoplasm vacuolation. Irregularity of the sarcolemma was also observed in the myocardial myocytes and could be attributed to the released free radicals that induced lipid peroxidation of the cellular membranes (Jia, Yang *et al.*, 2022, Shirmard, Shabani *et al.*, 2022).

In the ADMSCs-treated group, most of the myofibrils were organized and regularly arranged, branched, and exhibited elongated vesicular nuclei. These results indicated regression of most of the degenerative changes in the cardiac myocytes in response to MSCs therapy. This might be due to the noticeably improved levels of TAC and the reduced levels of MDA, TNF- α , and IL-2 in the cardiac tissue of animals treated with stem cells. These findings proposed that stem cells have

antioxidant and anti-inflammatory potential. The therapeutic effect of mesenchymal stem cells has been established on cardiac muscle repair, but there were controversial reports about the repair mechanisms (Wu, Zhao *et al.* 2010, Fukata, Ishikawa *et al.*, 2013, Lee, Lee *et al.*, 2014).

MSCs can differentiate into several cell lineages, including cardiomyocytes.

Several molecules are known to be involved in the tethering, rolling, adhesion, and transmigration of leukocytes from the bloodstream into tissues; these molecules include

integrins, selectins, and chemokine receptors are also expressed in MSCs (Rüster, Göttig *et al.*, 2006). Due to this feature, MSCs were reported to possess an immunomodulatory effect and could decrease the levels of inflammatory mediators and hence, become effective in treating inflammatory cardiac diseases (Van Linthout, Stamm *et al.*, 2011, Petryk and Shevchenko 2020). In addition, MSCs enhance the repair process by altering the inflammatory responses in the infarcted myocardium by secretory immunosuppressive soluble factors such as prostaglandin, E2 and IL-10 (Wang, Yuan *et al.*, 2018).

With the help of the secretion of various immunomodulators and by modulation of multiple functions of immune cells, MSCs exert their anti-inflammatory effects. As they can activate, suppress, and regulate the differentiation and migration of T and B lymphocytes, macrophages, natural killer cells, and neutrophils (Liotta, Angeli *et al.*, 2008, Weiss and Dahlke 2019).

ADMSCs were chosen in this study due to their minimal invasiveness, abundance, and ease of obtaining. Also, they could be cultured in sufficient numbers for autologous transplantation (Lin, Leu *et al.*, 2010). Furthermore, AD-MSCs expanded rapidly and were more resistant than Bone Marrow Mesenchymal Cells (BM -MSCs) to chemotherapy-induced cell senescence

and apoptosis, signifying their use in clinical application (Qi, Zhang *et al.*, 2012). Moreover, they can release superoxide dismutase, catalase, and glutathione peroxidase, which are hydrogen peroxide-scavenging enzymes. Also, they can provide resistance to oxidative stress-induced cell death (Valle-Prieto and Conget 2010).

The present study showed increased expression of VEGF immunoreactivity in the cisplatin-treated group in comparison to the control, which is an essential angiogenic marker. Upregulation of VEGF could be stimulated by hypoxia in degenerated areas (Maranhão, Guido *et al.*, 2017). Neovascularization is critical for tissue regeneration. A significant high expression of the VEGF marker in the MSCs-treated group was demonstrated. Similarly, (Tang, Xie *et al.* 2006) found an increased VEGF expression level after the transplantation of MSCs into the ischemic myocardium with reperfusion. Increased VEGF triggers the angiogenic progress of MSCs. Interestingly, they showed MSC differentiation into endothelial cells or cardiomyocytes, which was related to the presence of VEGF. An obvious increase in the density of blood capillaries and the cardiomyocytes' number-like cells were observed in degenerated areas after injecting ADMSCs. These changes could lead to improved cardiac function because of the improvement of the blood supply in damaged heart tissue.

The present findings demonstrated a decline of cardiac degeneration in ADMSCs-treated animals accompanied by down-regulation of caspase-3 immunoexpression. Apoptosis of cardiac myocytes exaggerates cardiac degeneration and progression to myocardial infarction, so anti-apoptotic treatment is recommended to decrease the degree of infarction. We postulate that these cells will act by this mechanism (Li, Zhang *et al.*, 2008).

Previous studies showed similar results after the transplantation of MSCs, which were attributed to released cytokines from MSCs and the upregulation of Bcl2 and its receptors (Mao, Lin *et al.* 2014, Chen, Lu *et al.*, 2016). Kim, Park *et al.* (2012) proposed that MSCs protect the kidney from cisplatin-induced apoptotic nephrotoxicity by a significantly decreased expression of caspase-3 that was mediated via inhibition of the mitochondrial apoptosis signaling pathway. The current study revealed negative expression of CD44+ve and CD105+ve cells in cisplatin and withdrawal groups. But after administration of ADMSCs, there was significant expression of both CD44+ve cells and CD105+ve cells compared to the cisplatin-treated group.

These stem /progenitor cells have a promising role in enhancing the regeneration of damaged cells, and numerous of these cells retrieved from adipose tissue exhibit surface markers positive for CD44, CD90, and CD105 (Arslan, Galata *et al.*, 2018). These findings indicated the homing mechanism of stem cells to the degenerated cardiac tissue and releasing cytokines (Li, Huang *et al.*, 2015). Moreover, the upregulation of the HLA-B gene in the MSCs-treated group in the current study supported homing theory. Homing process of stem cells could be related to the beginning of the inflammatory process and cytokines release (Hale, Dai *et al.*, 2008).

Conclusion

It could be concluded from the current findings that intravenous injection of AD-MSCs is accompanied by homing of the ADMSC into rat cardiac tissue that ameliorated the cardiotoxicity induced by cisplatin through inhibition of inflammatory and apoptotic cascades, suppression of oxidative stress, and activation of angiogenesis which might be due to homing rather than self-differentiation. ADMSCs could be a new therapeutic hope against chemotherapy-induced

cardiotoxicity. However, additional research should be done to support the current results and to monitor the differentiation of ADMSCs in order to assess their effectiveness and durability over time.

Acknowledgments:

We want to thank the Medical Research Centre (MRC) and the Tissue Culture and Molecular Biology (TCMB) lab for their means of keeping to most of our laboratory investigations.

Ethical Approval Statement:

The experiment's methods were carried out following the generally accepted guidelines for the care and use of laboratory animals and were approved by the faculty's ethics committee at Assiut University in Assiut, Egypt.

Declaration of Interest:All authors declare no related conflicts of interest.

Funding:Assiut University is the source of funding for this research.

REFERENCES

- Abushouk, A. I., A. M. A. Salem, A. M. Saad, A. Y. Afify, H. Afifi, A. Afifi, H. Salem, E. Ghanem and M. M. Abdel-Daim (2019). Mesenchymal stem cell therapy for doxorubicin-induced cardiomyopathy: potential mechanisms, governing factors, and implications of the heart stem cell debate. *Frontiers in Pharmacology*, 10: 635.
- Ali, F. E. M., E. H. M. Hassanein, A. H. El-Bahrawy, Z. M. M. Omar, E. K. Rashwan, B. A. Abdel-Wahab and T. H. Abd-Elhamid (2021). Nephroprotective effect of umbelliferone against cisplatin-induced kidney damage is mediated by regulation of NRF2, cytoglobin, SIRT1/FOXO-3, and NF- κ B-p65 signaling pathways. *Journal of Biochemical and Molecular Toxicology*, 35(5): e22738.
- Ammar, H. I., G. L. Sequiera, M. B. Nashed, R. I. Ammar, H. M. Gabr, H. E. Elsayed, N. Sareen, E. A. Rub, M. B. Zickri and S. Dhingra (2015). Comparison of adipose tissue- and bone marrow-derived mesenchymal stem cells for alleviating doxorubicin-induced cardiac dysfunction in diabetic rats. *Stem cell research & therapy*, 6(1): 148.
- Arslan, Y. E., Y. F. Galata, T. Sezgin Arslan and B. Derkus (2018). Trans-differentiation of human adipose-derived mesenchymal stem cells into cardiomyocyte-like cells on decellularized bovine myocardial extracellular matrix-based films. *Journal of Materials Science: Materials in Medicine*, 29(8): 127.
- Ateşşahin, A., I. Karahan, G. Türk, S. Gür, S. Yılmaz and A. O. Ceribaşı (2006). Protective role of lycopene on cisplatin-induced changes in sperm characteristics, testicular damage and oxidative stress in rats. *Reproductive Toxicology*, 21(1): 42-47.
- Bancroft, J. D. and M. Gamble (2008). Theory and practice of histological techniques, Elsevier health sciences.
- Beltrami, A. P., L. Barlucchi, D. Torella, M. Baker, F. Limana, S. Chimenti, H. Kasahara, M. Rota, E. Musso and K. Urbanek (2003). Adult cardiac stem cells are multipotent and support myocardial regeneration. *Cell*, 114(6): 763-776.
- Bukhari, I. A., O. Y. Mohamed, A. M. Alhowikan, R. Lateef, H. Hagar, R. A. Assiri and W. M. A. Alqahtani (2022). Protective Effect of Rutin Trihydrate Against Dose-Dependent, Cisplatin-Induced Cardiac Toxicity in Isolated Perfused Rat's Heart. *Cureus*, 14(1): e21572.
- Chen, C.-T., Z.-H. Wang, C.-C. Hsu, H.-H. Lin and J.-H. Chen (2015). In vivo protective effects of

- diosgenin against doxorubicin-induced cardiotoxicity. *Nutrients*, 7(6): 4938-4954.
- Chen, X., M. Lu, N. Ma, G. Yin, C. Cui and S. Zhao (2016). "Dynamic tracking of injected mesenchymal stem cells after myocardial infarction in rats: a serial 7T MRI study." *Stem Cells International*, 2016: 4656539.
- Chowdhury, S., K. Sinha, S. Banerjee and P. C. Sil (2016). Taurine protects cisplatin induced cardiotoxicity by modulating inflammatory and endoplasmic reticulum stress responses. *Biofactors*, 42(6): 647-664.
- Conklin, K. A. and G. L. Nicolson (2008). Molecular replacement in cancer therapy: reversing cancer metabolic and mitochondrial dysfunction, fatigue and the adverse effects of therapy. *Current Cancer Therapy Reviews*, 4: 66-76.
- El-Sawalhi, M. M. and L. A. Ahmed (2014). "Exploring the protective role of apocynin, a specific NADPH oxidase inhibitor, in cisplatin-induced cardiotoxicity in rats." *Chemico-biological interactions*, 207: 58-66.
- Francescato, H. D., R. S. Costa, C. Scavone and T. M. Coimbra (2007). Parthenolide reduces cisplatin-induced renal damage. *Toxicology*, 230(1): 64-75.
- Fukata, M., F. Ishikawa, Y. Najima, T. Yamauchi, Y. Saito, K. Takenaka, K. Miyawaki, H. Shimazu, K. Shimoda and T. Kanemaru (2013). Contribution of bone marrow-derived hematopoietic stem/progenitor cells to the generation of donor-marker+ cardiomyocytes in vivo. *PLoS One*, 8(5): e62506.
- Glauert, A. M. and P. R. Lewis (2014). Biological specimen preparation for transmission electron microscopy. *Biological Specimen Preparation for Transmission Electron Microscopy*, Princeton University Press.
- Hale, S. L., W. Dai, J. S. Dow and R. A. Kloner (2008). Mesenchymal stem cell administration at coronary artery reperfusion in the rat by two delivery routes: a quantitative assessment. *Life sciences*, 83(13-14): 511-515.
- Hassan, A. I. and S. S. Alam (2014). Evaluation of mesenchymal stem cells in treatment of infertility in male rats. *Stem cell research & therapy*, 5(6): 131.
- Hideg, K. and T. Kálai (2007). Novel antioxidants in anthracycline cardiotoxicity. *Cardiovascular toxicology*, 7(2): 160-164.
- Huang, C., X. Zhang, J. M. Ramil, S. Rikka, L. Kim, Y. Lee, N. A. Gude, P. A. Thistlethwaite, M. A. Sussman and R. A. Gottlieb (2010). Juvenile exposure to anthracyclines impairs cardiac progenitor cell function and vascularization resulting in greater susceptibility to stress-induced myocardial injury in adult mice. *Circulation*, 121(5): 675.
- Huang, J., Y. Lei, S. Lei and X. Gong (2022). Cardioprotective effects of corilagin on doxorubicin induced cardiotoxicity via P13K/Akt and NF-κB signaling pathways in a rat model. *Toxicology Mechanisms and Methods*, 32(2): 79-86.
- Ibrahim, M. A., G. A. Bakhaat, H. G. Tammam, R. M. Mohamed and S. A. El-Naggar (2019). Cardioprotective effect of green tea extract and vitamin E on Cisplatin-induced cardiotoxicity in mice: toxicological, histological and immunohistochemical studies. *Biomedicine & Pharmacotherapy*, 113: 108731.

- Jang, Y., J. Choi, N. Park, J. Kang, M. Kim, Y. Kim and J. H. Ju (2019). Development of immunocompatible pluripotent stem cells via CRISPR-based human leukocyte antigen engineering. *Experimental & Molecular Medicine*, 51(1): 1-11.
- Jia, L., L. Yang, Y. Tian, L. Yang, D. Wu, H. Zhang, M. Li and N. Wu (2022). Nrf2 participates in the protective effect of exogenous mitochondria against mitochondrial dysfunction in myocardial ischaemic and hypoxic injury. *Cellular Signalling*, 92: 110266.
- Johnson, J., S. Mohsin and S. R. Houser (2021). Cardiomyocyte Proliferation as a Source of New Myocyte Development in the Adult Heart. *International Journal of Molecular Sciences*, 22(15):7764.
- Jomova, K. and M. Valko (2011). Advances in metal-induced oxidative stress and human disease. *Toxicology*, 283(2-3): 65-87.
- Kim, J.-S., L. He and J. J. Lemasters (2003). Mitochondrial permeability transition: a common pathway to necrosis and apoptosis. *Biochemical and biophysical research communications*, 304(3): 463-470.
- Kim, J. H., D. J. Park, J. C. Yun, M. H. Jung, H. D. Yeo, H.-J. Kim, D. W. Kim, J. I. Yang, G.-W. Lee and S.-H. Jeong (2012). Human adipose tissue-derived mesenchymal stem cells protect kidneys from cisplatin nephrotoxicity in rats. *American Journal of Physiology-Renal Physiology*, 302(9): F1141-F1150.
- Kobayashi, C. I. and T. Suda (2012). Regulation of reactive oxygen species in stem cells and cancer stem cells. *Journal of cellular physiology*, 227(2): 421-430.
- Koracevic, D., G. Koracevic, V. Djordjevic, S. Andrejevic and V. Cosic (2001). Method for the measurement of antioxidant activity in human fluids. *Journal of clinical pathology*, 54(5): 356-361.
- Lee, J.-W., S.-H. Lee, Y.-J. Youn, M.-S. Ahn, J.-Y. Kim, B.-S. Yoo, J. Yoon, W. Kwon, I.-S. Hong and K. Lee (2014). A randomized, open-label, multicenter trial for the safety and efficacy of adult mesenchymal stem cells after acute myocardial infarction. *Journal of Korean medical science*, 29(1): 23-31.
- Li, L., Y. Zhang, Y. Li, B. Yu, Y. Xu, S. Zhao and Z. Guan (2008). Mesenchymal stem cell transplantation attenuates cardiac fibrosis associated with isoproterenol-induced global heart failure. *Transplant International*, 21(12): 1181-1189.
- Li, S., K.-J. Huang, J.-C. Wu, M. S. Hu, M. Sanyal, M. Hu, M. T. Longaker and H. P. Lorenz (2015). Peripheral blood-derived mesenchymal stem cells: Candidate cells responsible for healing critical-sized calvarial bone defects. *Stem cells translational medicine*, 4(4): 359-368.
- Lian, Y., L. Gao, P. Guo, Y. Zhao and T. Lin (2016). Grape seed proanthocyanidins extract prevents cisplatin-induced cardiotoxicity in rats. *Food Science and Technology Research*, 22(3): 403-408.
- Lin, Y.-C., S. Leu, C.-K. Sun, C.-H. Yen, Y.-H. Kao, L.-T. Chang, T.-H. Tsai, S. Chua, M. Fu and S.-F. Ko (2010). Early combined treatment with sildenafil and adipose-derived mesenchymal stem cells

- preserves heart function in rat dilated cardiomyopathy. *Journal of translational medicine*, 8(1): 88.
- Liotta, F., R. Angeli, L. Cosmi, L. Filì, C. Manuelli, F. Frosali, B. Mazzinghi, L. Maggi, A. Pasini and V. Lisi (2008). Toll-like receptors 3 and 4 are expressed by human bone marrow-derived mesenchymal stem cells and can inhibit their T-cell modulatory activity by impairing Notch signaling. *Stem cells*, 26(1): 279-289.
- Livak, K. J. and T. D. Schmittgen (2001). Analysis of relative gene expression data using real-time quantitative PCR and the 2- $\Delta\Delta$ CT method. *Methods*, 25(4): 402-408.
- Maliken, B. D. and J. D. Molkenin (2018). Undeniable evidence that the adult mammalian heart lacks an endogenous regenerative stem cell. *Circulation*, 138(8): 806-808.
- Mao, Q., C. Lin, J. Gao, X. Liang, W. Gao, L. Shen, L. Kang and B. Xu (2014). Mesenchymal stem cells overexpressing integrin-linked kinase attenuate left ventricular remodeling and improve cardiac function after myocardial infarction. *Molecular and Cellular Biochemistry*, 397(1-2): 203-214.
- Maranhão, R. C., M. C. Guido, A. D. de Lima, E. R. Tavares, A. F. Marques, M. D. T. de Melo, J. C. Nicolau, V. M. Salemi and R. Kalil-Filho (2017). Methotrexate carried in lipid core nanoparticles reduces myocardial infarction size and improves cardiac function in rats. *International journal of nanomedicine*, 12: 3767.
- Marra, C., A. Bizzarro, A. Daniele, L. De Luca, M. Ferraccioli, A. Valenza, C. Brahe, F. D. Tiziano, G. Gainotti and C. Masullo (2004). Apolipoprotein E ϵ 4 allele differently affects the patterns of neuropsychological presentation in early- and late-onset Alzheimer's disease patients. *Dementia and geriatric cognitive disorders*, 18(2): 125-131.
- Martínez-Mateo, V., M. Anguita, L. Del Campo and A. Paule-Sánchez (2017). "A Case Report of Cisplatin-Induced Cardiotoxicity: A Side Effect to Monitor Closely. *Journal of Heart Health*, 3(2):2379-769.
- Mathur, A., F. Fernández-Avilés, S. Dimmeler, C. Hauskeller, S. Janssens, P. Menasche, W. Wojakowski, J. F. Martin, A. Zeiher and B. Investigators (2017). The consensus of the Task Force of the European Society of Cardiology concerning the clinical investigation of the use of autologous adult stem cells for the treatment of acute myocardial infarction and heart failure: update 2016. *European heart journal*, 38(39): 2930-2935.
- Mazini, L., L. Rochette, M. Amine and G. Malka (2019). Regenerative capacity of adipose derived stem cells (ADSCs), comparison with mesenchymal stem cells (MSCs). *International journal of molecular sciences*, 20(10): 2523.
- Meligy, F. Y., H. S. El-Deen Mohammed, T. M. Mostafa, M. M. Elfiky, I. El-Sayed Mohamed Ashry, A. M. Abd-Eldayem, N. I. Rizk, D. Sabry, E. S. H. Abd Allah and S. F. Ahmed (2022). Therapeutic Potential of Mesenchymal Stem Cells versus Omega n - 3 Polyunsaturated Fatty Acids on Gentamicin-Induced Cardiac

- Degeneration. *Pharmaceutics*, 14(7):1322.
- Meligy, F. Y., K. Shigemura, H. M. Behnsawy, M. Fujisawa, M. Kawabata and T. Shirakawa (2012). The efficiency of in vitro isolation and myogenic differentiation of MSCs derived from adipose connective tissue, bone marrow, and skeletal muscle tissue. *In Vitro Cellular & Developmental Biology-Animal*, 48(4): 203-215.
- Murphy, S. V. and A. Atala (2013). Amniotic fluid stem cells. *Perinatal stem cells*, 1-15.
- Nakagawa, H., S. Akita, M. Fukui, T. Fujii and K. Akino (2005). Human mesenchymal stem cells successfully improve skin-substitute wound healing. *British Journal of Dermatology*, 153(1): 29-36.
- Pelacho, B., X. L. Aranguren, M. Mazo, G. Abizanda, J. J. Gavira, C. Clavel, M. Gutierrez-Perez, A. Luttun, C. M. Verfaillie and F. Prósper (2007). Plasticity and cardiovascular applications of multipotent adult progenitor cells. *Nature Clinical Practice Cardiovascular Medicine*, 4(1): S15-S20.
- Petryk, N. and O. Shevchenko (2020). Mesenchymal stem cells anti-inflammatory activity in rats: Proinflammatory Cytokines. *Journal of Inflammation Research*, 13: 293.
- Pınarlı, F. A., N. N. Turan, F. Güçlü Pınarlı, A. Okur, D. Sönmez, T. Ulus, A. Oğuz, C. Karadeniz and T. Delibaşı (2013). Resveratrol and adipose-derived mesenchymal stem cells are effective in the prevention and treatment of doxorubicin cardiotoxicity in rats. *Pediatric hematology and oncology*, 30(3): 226-238.
- Qi, Z., Y. Zhang, L. Liu, X. Guo, J. Qin and G. Cui (2012). Mesenchymal stem cells derived from different origins have unique sensitivities to different chemotherapeutic agents. *Cell biology international*, 36(9): 857-862.
- Qian, W., M. Nishikawa, A. M. Haque, M. Hirose, M. Mashimo, E. Sato and M. Inoue (2005). Mitochondrial density determines the cellular sensitivity to cisplatin-induced cell death. *American Journal of Physiology-Cell Physiology*, 289(6): C1466-C1475.
- Refaie, M. M., M. El-Hussieny, A. M. Bayoumi, S. Shehata, N. N. Welson and W. Y. Abdelzaher (2022). Simvastatin cardioprotection in cyclophosphamide -induced toxicity via the modulation of inflammasome/caspase1/interleukin1 β pathway. *Human and Experimental Toxicology*, 41: 9603271221111440.
- Rüster, B., S. Göttig, R. J. Ludwig, R. Bistran, S. Müller, E. Seifried, J. Gille and R. Henschler (2006). Mesenchymal stem cells display coordinated rolling and adhesion behavior on endothelial cells. *Blood*, 108(12): 3938-3944.
- Sherif, I. O., A. Abdel-Aziz and O. M. Sarhan (2014). Cisplatin-induced testicular toxicity in rats: the protective effect of arjunolic acid. *Journal of biochemical and molecular toxicology*, 28(11): 515-521.
- Shirmard, L. R., M. Shabani, A. A. Moghadam, N. Zamani, H. Ghanbari and A. Salimi (2022). Protective Effect of Curcumin, Chrysin and Thymoquinone Injection on Trastuzumab-Induced Cardiotoxicity via Mitochondrial Protection. *Cardiovascular Toxicology*, 1-13.
- Tang, J., Q. Xie, G. Pan, J. Wang and M. Wang (2006). Mesenchymal stem cells participate in

- angiogenesis and improve heart function in rat model of myocardial ischemia with reperfusion. *European Journal of Cardio-Thoracic Surgery*, 30(2): 353-361.
- Topal, İ., A. Ö. Bilgin, F. K. Çimen, N. Kurt, Z. Süleyman, Y. Bilgin, A. Özçiçek and D. Altuner (2018). The effect of rutin on cisplatin-induced oxidative cardiac damage in rats. *Anatolian Journal of Cardiology*, 20(3): 136.
- Valle-Prieto, A. and P. A. Conget (2010). Human mesenchymal stem cells efficiently manage oxidative stress. *Stem cells and development* 19(12): 1885-1893.
- Van Linthout, S., C. Stamm, H.-P. Schultheiss and C. Tschöpe (2011). Mesenchymal stem cells and inflammatory cardiomyopathy: cardiac homing and beyond. *Cardiology research and practice*, 2011.
- Varga, Z. V., P. Ferdinandy, L. Liaudet and P. Pacher (2015). Drug-induced mitochondrial dysfunction and cardiotoxicity. *American Journal of Physiology-Heart and Circulatory Physiology*, 309(9): H1453-H1467.
- Varricchi, G., P. Ameri, C. Cadeddu, A. Ghigo, R. Madonna, G. Marone, V. Mercurio, I. Monte, G. Novo and P. Parrella (2018). Antineoplastic drug-induced cardiotoxicity: a redox perspective. *Frontiers in Physiology*, 9: 167.
- Večerić-Haler, Ž., A. Cerar and M. Perše (2017). "(Mesenchymal) Stem cell-based therapy in cisplatin-induced acute kidney injury animal model: risk of immunogenicity and tumorigenicity. *Stem cells international*, 2017.
- Wang, M., Q. Yuan and L. Xie (2018). Mesenchymal stem cell-based immunomodulation: properties and clinical application. *Stem cells international, Stem Cells International*, 14;2018:3057624 . doi: 10.1155/ 2018/ 3057624
- Weiss, A. R. R. and M. H. Dahlke (2019). Immunomodulation by Mesenchymal Stem Cells (MSCs): Mechanisms of Action of Living, Apoptotic, and Dead MSCs. *Frontiers in Immunology*, 10: 1191.
- Wu, Y., R. C. Zhao and E. E. Tredget (2010). Concise review: bone marrow-derived stem/progenitor cells in cutaneous repair and regeneration. *Stem cells*, 28(5): 905-915.

ARABIC SUMMARY

الخلايا الجذعية الدهنية للأنسجة الوسيطة تعمل على تحسين السمية القلبية التي يسببها السيسبلاتين في الجرذان عن طريق تعديل موت الخلايا المبرمج والإجهاد التأكسدي والالتهاب وتكوين الأوعية الدموية

أمل راتب^{1*}، أسماء جمعة²، علا حسين³

¹ قسم التشريخ الأدمى والأجنة، ² قسم الفسيولوجيا الطبية، ³ قسم الهستولوجيا وبيولوجيا الخلية، كلية الطب، جامعة أسبوط، أسبوط، مصر

الخلفية: السمية القلبية من الآثار الجانبية المتكررة للعلاج بالسيسبلاتين. والى الآن لم يتم توضيح آليات السمية القلبية التي يسببها السيسبلاتين بوضوح. ولقد تم التعرف على الخلايا الجذعية كإستراتيجية علاجية مبتكرة مفيدة محتملة في العديد من الأمراض.

الهدف: تم تصميم الدراسة الحالية لتقييم تأثير الخلايا الجذعية الوسيطة الدهنية (ADMSCs) ضد الأضرار القلبية التي يسببها السيسبلاتين والتحقيق في آليات العمل الممكنة.

المواد وطرق البحث: تم تصنيف اثنان وثلاثون جرزا عشوائيا إلى أربع مجموعات متساوية: المجموعة الضابطة والتي تلقت محلول ملحي حقنا في التجوف البريتوني، المجموعة المعالجة بالسيسبلاتين والتي تلقت جرعة واحدة من السيسبلاتين بجرعة 7 مجم / كجم حقنا في التجوف البريتوني ثم تركت لمدة خمسة أيام، المجموعة المعالجة بالخلايا الجذعية التي أعطت السيسبلاتين وبعد 5 أيام تلقوا جرعة واحدة من الخلايا الجذعية الدهنية للأنسجة الوسيطة (1×10^6) مل حقنا في الوريد ولقد تركت لمدة ستون يوماً اخري من حقن الخلايا، ومجموعة الانسحاب والتي تلقت السيسبلاتين ثم تركت لمدة خمسة وستون يوماً.

بنهاية التجربة، تم استخدام جزء من أنسجة القلب لتحديد مستويات السعة الكلية لمضادات الأوكسدة (TAC)، والمالونديالدهيد (MDA)، وعامل نخر الورم ألفا ($TNF-\alpha$) والإنترلوكين 2- (IL) في أنسجة القلب. ثم تم تحضير الأجزاء المتبقية من عضلة القلب للدراسات النسيجية والهستوكيميائية المناعية.

النتائج: أظهرت نتائج هذه الدراسة التأثير المدمر للسيسبلاتين على عضلة القلب حيث لوحظ ان عضلة القلب قد فقدت انتظام ترتيب الألياف العضلية مع تهتك وتحلل لمعظم هذه الألياف العضلية، التي بدت منفصلة على نطاق واسع. كذا ظهرت الأنوية مشوهة بشدة و بدت شديدة التكتيف وشكلها غير منتظم مع تغيرات شديدة في الميتوكوندريا. أما بالنسبة لمستويات السيتوكينات المنشطة للالتهابات فقد أوضحت النتائج زيادة عامل نخر الورم ألفا $TNF-\alpha$ والإنترلوكين 2- IL في الأنسجة القلبية للجرذان مع ارتفاع مستوى المالونديالدهيد و انخفاض مستوى السعة الكلية لمضادات الأوكسدة. TAC في حين أدى حقن الخلايا الجذعية الدهنية للأنسجة الوسيطة إلى تحسين السمية القلبية التي يسببها السيسبلاتين من خلال قمع الإجهاد التأكسدي، وتثبيط السيتوكينات الالتهابية، وقمع شلالات موت الخلايا المبرمج، وتفعيل تكوين الأوعية.

الخلاصة: العلاج باستخدام الخلايا الجذعية الدهنية للأنسجة الوسيطة له دور واعد لتعزيز التجديد الملحوظ لإصابة عضلة القلب التي يسببها السيسبلاتين.